HHS Public Access

Author manuscript

Inhal Toxicol. Author manuscript; available in PMC 2023 January 24.

Published in final edited form as:

Inhal Toxicol. 2022 ; 34(9-10): 275–286. doi:10.1080/08958378.2022.2089783.

Lung toxicity profile of inhaled copper-nickel welding fume in A/J mice

Patti C. Zeidler-Erdely[a], **Aaron Erdely**[a], **Vamsi Kodali**[a], **Ronnee Andrews**[a], **James Antonini**[a], **Taylor Trainor-DeArmitt**[a], **Rebecca Salmen**[a], **Lori Battelli**[a], **Lindsay Grose**[a], **Michael Kashon**[a], **Samantha Service**[a], **Walter McKinney**[a], **Samuel Stone**[a], **Lauryn Falcone**[b]

[a]Health Effects Laboratory Division, National Institute for Occupational Safety and Health, Morgantown, WV, USA

[b]Department of Dermatology, University of Pittsburgh Medical Center, Pittsburgh, PA, USA

Abstract

Objective: Stainless steel welding creates fumes rich in carcinogenic metals such as chromium (Cr). Welding consumables devoid of Cr are being produced in an attempt to limit worker exposures to toxic and carcinogenic metals. The study objective was to characterize a copper-nickel (Cu-Ni) fume generated using gas metal arc welding (GMAW) and determine the pulmonary deposition and toxicity of the fume in mice exposed by inhalation.

Materials and Methods: Male A/J mice (6–8 weeks of age) were exposed to air or Cu-Ni welding fumes for 2 (low deposition) or 4 (high deposition) hours/day for 10 days. Mice were sacrificed, and bronchoalveolar lavage (BAL), macrophage function, and histopathological analyses were performed at different timepoints post-exposure to evaluate resolution.

Results and Discussion: Characterization of the fume indicated that most of the particles were between 0.1 and 1 μm in diameter, with a mass median aerodynamic diameter of 0.43 μm. Metal content of the fume was Cu (~76%) and Ni (~12%). Post-exposure, BAL macrophages had a reduced ability to phagocytose E. coli, and lung cytotoxicity was evident and significant (>12%–19% fold change). Loss of body weight was also significant at the early timepoints. Lung inflammation, the predominant finding identified by histopathology, was observed as a subacute response early that progressively resolved by 28 days with only macrophage aggregates remaining late (84 days).

Conclusions: Overall, there was high acute lung toxicity with a resolution of the response in mice which suggests that the Cu-Ni fume may not be ideal for reducing toxic and inflammatory lung effects.

CONTACT Patti C. Zeidler-Erdely, paz9@cdc.gov, National Institutes for Occupational Safety and Health, Health Effects Laboratory Division, 1000 Frederick Lane, Morgantown, WV 26508, USA.

Disclaimer

The findings and conclusions in this report are those of the authors and do not necessarily represent the official position of the National Institute for Occupational Safety and Health, Centers for Disease Control and Prevention. Mention of brand name does not constitute product endorsement.

Disclosure statement

No potential conflict of interest was reported by the author(s).

Keywords

Copper; welding; lung; strain A

Introduction

Welding, a method of joining metals, employs millions of workers around the world (IARC Working Group on the Evaluation of Carcinogenic Risk to Humans 2018). However, many types of welding produce significant amounts of fumes which are known to be hazardous to human health (Antonini 2003). Acute and chronic conditions such as metal fume fever, bronchitis, and increased infection incidence have been reported in welders (Coggon et al. 1994; Holm et al. 2012; Marongiu et al. 2016; Suri et al. 2016). Welding fumes may also cause lung cancer and are classified as *carcinogenic to humans* (Group 1) by the International Agency for Research on Cancer (IARC) (IARC Working Group on the Evaluation of Carcinogenic Risk to Humans 2018). Hexavalent chromium (Cr^{6+}), also a Group 1 carcinogen, present in certain welding fumes is often considered to be the most pneumotoxic component metal (IARC Working Group on the Evaluation of Carcinogenic Risk to Humans 2012). In 2006, the Occupational Safety and Health Administration (OSHA) reduced the permissible Cr^{6+} concentration in the workplace from 52 to 5 ug/m^3. This reduction can be challenging to maintain with stainless steel (SS) welding. For this reason, newer welding consumables containing primarily copper (Cu) with some nickel (Ni) have been produced that may prove less hazardous to workers' health.

Epidemiological studies have investigated lung cancer after exposure to both mild steel (MS) and SS welding fumes. The former is composed almost entirely of iron (Fe) and manganese (Mn), while the latter contains Fe, Ni, Cr, Cu, and Mn. Most notably, worker studies suggest that both MS and SS fume exposures increase lung cancer in welders, even though MS fume contains no classified human carcinogens (Sorensen et al. 2007; Siew et al. 2008; 't Mannetje et al. 2012; Matrat et al. 2016). There are no epidemiological studies investigating worker exposure to fume from the newer Cu-Ni welding consumables and only limited *in vivo* and *in vitro* studies on the pneumotoxicity of the fume are available (Antonini et al. 2014; Badding et al. 2014).

The aim of this study was to investigate the lung toxicity profile following whole-body inhalation of a Cu-Ni welding fume at a low deposition (LD; 2 h/day for 10 days) or high deposition (HD; 4 h/day for 10 days) at a target concentration of 40 mg/m^3 in A/J mice. The A/J mouse is a lung tumor susceptible strain that will serve as a model for subsequent carcinogenicity studies for this fume as previously done (Zeidler-Erdely et al. 2013; Falcone et al. 2017; Falcone et al. 2018). The results of this study directly address acute and sub-chronic outcomes to clarify if Cu-Ni welding consumables could be safer workplace alternatives.

Methods

Animals

Male A/J mice (age 4–6 weeks) were purchased from Jackson Laboratories (Bar Harbor, ME) and housed in an Association for Assessment and Accreditation of Laboratory Animal Care (AAALAC) International - specific pathogen-free, environmentally-controlled facility. All mice were free of endogenous pathogens including viruses, bacteria, mycoplasmas, and parasites. Mice were housed in groups of two in ventilated cages and provided high-efficiency particulate filtered air under a controlled light cycle (12 h light/12 h dark) at a standard temperature (22°–24 °C) and 30%–70% relative humidity. Animals were acclimated to the animal facility for one week before beginning the experimental protocol and allowed access to a conventional diet (6% irradiated NIH-31 Diet, Envigo RMS, Inc.; Madison, WI) and tap water *ad libitum.* Male mice were chosen for this study in lieu of females because welding is a male-dominated profession. Approximately ~95% of welders are male according to the American Welding Society (https://weldingworkforce-data.com). All procedures were performed using protocols approved by the Centers for Disease Control Morgantown Institutional Animal Care and Use Committee.

Welding fume inhalation exposure system

The design and construction of the welding fume aerosol generator were previously described (Antonini et al. 2006). This automated robotic welder continuously generated welding fumes by welding beads onto ¼ inch thick plates of mild steel. The welding wire used was 0.045 inch diameter Lincoln Electric Techalloy 413 MIG (Lincoln Electric; Cleveland, OH), and the welding parameters were set to 25 volts DC, 300 inch per minute wire feed, 30 L/min of 75% argon −25% helium shielding gas, and a typical welding current of 200 amps. The resulting fume was carried into a whole-body exposure chamber through a ¾ inch flexible tube by maintaining the chamber at a negative pressure (0.70 inch H_2O). Particle concentrations within the exposure chamber were continuously monitored with a Data RAM (DR-40000 Thermo Electron Co; Franklin, MA), and gravimetric determinations (37 mm cassettes with 0.45 μm poresize Teflon filters) were used to calibrate and verify the Data RAM readings each day. Gas generation, including carbon monoxide (CO), carbon dioxide (CO_2), oxygen (O_2), and ozone (O_3), temperature and humidity were continuously monitored in the chamber. Average temperature and relative humidity were 72.0 ± 1.0 °F and 45.0 ± 11%, respectively, for all exposures. Approximately ten air changes per hour were done in the exposure chamber. During the welding exposure, O_2 levels were maintained above the OSHA minimal acceptable level. O_3, CO, CO_2 were below OSHA permissible exposure limits and National Institute for Occupational Safety and Health (NIOSH) recommended exposure limits (REL) during the entire exposure duration. In the exposure chamber, CO and O_3 levels were not significantly higher than background. The exposure system was modified slightly from that described previously to reduce the travel time of the particulate fume from the welding torch to the exposure chamber.

Welding fume characterization

For elemental analysis of Cu-Ni fume, generated particles were collected inside the exposure chamber onto 5.0 μm polyvinyl chloride membrane filters in 37 mm cassettes during three

30 min collection periods. The particle samples were digested and the metals determined by Inductively Coupled Plasma Atomic Emission Spectroscopy (ICP-AES) according to the NIOSH Manual of Analytical Methods (NMAM) method 7303 for hot block/HCl/HNO_3 digestion (NIOSH 1994). The welding fume was analyzed for aluminum (Al), barium (Ba), calcium (Ca), Cr, cobalt (Co), copper (Cu), Fe, potassium (K), lithium (Li), Mn, magnesium (Mg), Ni, phosphorus (P), lead (Pb), strontium (Sr), titanium (Ti), vanadium (V), zinc (Zn), and zirconium (Zr).

A small amount of welding fume was collected gravimetrically onto 47 mm Nucleopore polycarbonate filters (Whatman; Clinton, PA) for field emission scanning electron microscopy (FESEM) to assess particle size and morphology. The particles were imaged using a Hitachi S4800 Field Emission Scanning Electron Microscope (Hitachi; Tokyo, Japan). To determine particle mass size distribution, a Micro-Orifice Uniform Deposit Impactor (MOUDI, model 110; MSP corp., Shoreview, MN) with additional Nano-MOUDI stages (MSP model 115) was used. Elemental profiles of collected welding fume samples were determined using energy dispersive X-ray analysis (SEM-EDS; Princeton Gamma-Tech, Rocky Hill, NJ) at 20 keV to map specific metal components.

Whole lung metal analysis

Weight-matched A/J mice (age 5–7 weeks) were exposed by whole-body inhalation in individual steel mesh cages to Cu-Ni welding aerosols (mean concentration 43 mg/m^3) for 4 h ($n = 10$) or filtered air ($n = 6$). Immediately following exposure (time zero), mice were euthanized with sodium pentobarbital [100–300 mg/kg IP] (Vortech Pharmaceuticals; Dearborn, MI) followed by exsanguination via the vena cava. Whole lungs were excised, trimmed, and lyophilized. The freeze-dried tissue was weighed then acid digested. ICP-AES was used to determine the amount of Al, Ba, Ca, Co, Cr, Cu, Fe, K, Li, Mg, Mn, Ni, P, Pb, Sr, Ti, V, Zn and Zr present in the lung according to the NIOSH method 8200 used for bulk tissue samples (NIOSH 2018).

Experimental protocol for assessment of lung toxicity

Weight-matched A/J mice (5–7 weeks) were exposed by whole-body inhalation to Cu-Ni welding fume aerosols for 2 [LD; $n = 7–8$] or 4 h/day [HD; $n = 9–11$] for 10 days at a target concentration of 40 mg/m^3 (actual mean concentrations and standard deviations were 23 ± 8.8 and 27.3 ± 3.2 mg/m^3; respectively). Controls were exposed to filtered air [$n = 7–8$ (LD) or $n = 10–11$ (HD)]. One day before the start of the inhalation exposure mice were weight-matched, then weighed biweekly and again on the day of the terminal sacrifices of 1, 7, 28, and 84 days after the 10 day exposure. Body weights were determined by placing the conscious animal into a weight container on a calibrated digital balance. Mice were euthanized as described above.

For whole lung bronchoalveolar lavage, a blunted cannula was placed in the trachea through a small incision, and the thorax was massaged as 0.6 mL of cold Ca^{2+} and Mg^{2+} -free phosphate buffered saline (PBS) was instilled into the lungs. After 10 s, the BAL fluid was withdrawn and placed in a 15 ml conical tube. This consisted of the first lavage fraction. This process was then repeated three times (1 ml PBS/instillate), and this second fraction

was collected in a separate 15-ml conical tube. The BAL fluid was kept on ice and then centrifuged (500 × g, 10 min, 4 °C).

Lung toxicity parameters

LDH activity, indicative of lung cytotoxicity, was measured in the first fraction BAL supernatant. LDH activity was analyzed using a COBAS MIRA Plus auto-analyzer (Roche Diagnostic Systems; Montclair, NJ) which measured the oxidation of lactate to pyruvate coupled with the formation of NADH at 340 nm.

For analysis of the BAL cells, the supernatant from the second lavage fraction was discarded and the cell pellets of both fractions were combined. The final cell pellet suspended in 800 μl of PBS was used for cell counts and differential staining. Total cell numbers were determined using a hemocytometer. For cell differentials, cells were plated onto glass slides using a Cytospin 3 centrifuge (Shandon Life Sciences International; Cheshire, England) set at 800 rpm for 5 min. Slides were stained with Hema 3 Fixative and Solutions (Fisher Scientific; Pittsburgh, PA) then cover-slipped. A minimum of 300 cells/slide, consisting of macrophages, lymphocytes, and polymorphonuclear leukocytes, were identified using light microscopy.

Macrophage functional assay

The macrophage functional assay was done to examine the effect of the Cu-Ni LD fume exposure on innate immune function. Alveolar macrophages harvested by BAL at 1, 7, and 28 days post-exposure were challenged with *Escherichia coli* (*E. coli*) green fluorescent protein (GFP) for 2 h at 1:25 multiplicity of infection (Kodali et al. 2017). Macrophages from the lavage were enriched by surface adhesion as previously described (Driscoll et al. 1990; Yang et al. 1999; Ma et al. 2011). Briefly, the macrophages in the BAL were quantified by hemocytometer and resuspended in Eagle Minimum Essential Medium (EMEM, Lonza BioWhittaker, Walkersville, MD) containing 2 mM glutamine, 100 μg/ml streptomycin, 100 U/ml penicillin, 5 mM HEPES, and 10% heat-inactivated FBS at 5.0 × 10^5 cells/ml. The cell suspension (0.5 ml) was plated in a 24 well plate and allowed to adhere for 3 h in a humidified incubator (37 °C and 5% CO_2). After 3 h, adherent monolayers were rinsed vigorously three times with media. *E. coli* GFP (ATCC, VA, USA; #25922GFP) were cultured at 37 °C, 150 rpm for 6 h in sterile LB Miller Broth (Fisher Scientific, NH, USA; #BP1426500) supplemented with 100 μg/ml of ampicillin to maintain selection pressure of the GFP. After 6 h of culture, the bacteria were washed with PBS by centrifugation at 2000 rpm for 5 min and resuspended in EMEM (maintained at 4 °C). The surface adhesion enriched alveolar macrophages were then challenged with GFP *E. Coli.* After 2 h, the cells were washed with PBS, harvested by trypsinization and scraping, centrifuged at 1000 g for 5 min and resuspended in PBS. The cell-associated bacteria were quantified using a BD LSR II flow cytometer (BD Biosciences, San Diego, CA). The mean fluorescence was determined using FlowJo (FlowJo LLC, Ashland, Oregon). The uptake of *E.coli* by macrophages was quantified by flow cytometry.

Cytokine/chemokine BAL fluid analysis

Cytokine concentrations from the first fraction BAL supernatant at 7 day and 28 days post-exposure were quantified simultaneously by using the Discovery Assay Mouse Cytokine Array/Chemokine Array 32-Plex (Eve Technologies Corp; Calgary, AB, CA). The multiplex assay was performed at Eve Technologies using the Bio-Plex 200 system (Bio-Rad Laboratories, Inc.; Hercules, CA), and a Milliplex Mouse Cytokine/Chemokine kit (Millipore; St. Charles, MO) according to their protocol. The 32-plex consisted of eotaxin, granulocyte-colony stimulating factor (G-CSF), granulocyte monocyte-colony stimulating factor (GM-CSF), interferon gamma (IFNγ), interleukin-1α (IL-1α), IL-1β, IL-2, IL-3, IL-4, IL-5, IL-6, IL-7, IL-9, IL-10, IL-12 (p40), IL-12 (p70), IL-13, IL-15, IL-17, IFN-γ-inducible protein 10 (IP-10), keratinocyte chemoattractant (KC), leukemia inhibitory factor (LIF), C-X-C motif chemokine 5 (CXCL5), monocyte chemotactic protein 1 (MCP-1), macrophage-colony stimulating factor (M-CSF), monokine induced by gamma interferon (MIG), macrophage inflammatory protein-1α (MIP-1α), MIP-1 β, MIP-2, regulated on activation, normal T-cell expressed and secreted (RANTES), tumor necrosis factor-α (TNF-α), and vascular endothelial growth factor (VEGF). Standard curves with a range of 0 to >25,000 pg/ml were determined for each cytokine. A transformation of the limit of detection (LOD) was used for any value that was out of range. The assay sensitivities of the analytes ranged from 0.1–33.3 pg/ml.

Histopathological analysis

A separate set of animals, exposed simultaneously with the mice for the lung toxicity assays, were used for histopathology analysis. Mice were euthanized with sodium pentobarbital [100–300 mg/kg IP] (Vortech Pharmaceuticals; Dearborn, MI) followed by exsanguination via the vena cava. The right lung from the Cu-Ni HD exposure group [$n = 5$ (1 day); $n = 6$ (7, 28, 84 day)] or air controls [$n = 4$ (1 day); $n = 6$ (7, 28, 84 day)] was inflated in 10% neutral buffered formalin, then embedded in paraffin, and a 5 μm standardized section was cut. The left lung was frozen at −80 °C for future analysis. The slides were stained with hematoxylin and eosin and interpreted by a contracted board-certified veterinary pathologist. Histopathologic lesions were classified using standard published International Harmonization of Nomenclature and Diagnostic Criteria for Lesions (INHAND) terminology to the extent possible (Renne et al. 2009). Any histopathologic findings in the right lungs were graded and recorded using the following grading scale derived from Mann et al. 2012 as follows: No Visible Lesion [(NVL) tissue considered to be normal, under the conditions of the study and the strain of the animal)], 1 = minimal (the amount of change present barely exceeds that which is considered within normal limits), 2 = mild (In general, the lesion is easily identified but of limited severity), 3 = moderate (lesion is prominent, but there is significant potential for increased severity), 4 = marked [(the degree of change is as complete as possible (i.e. occupies much of the organ)].

Statistical comparisons and analysis

Statistical analyses were performed using RStudio Version 1.2.5001. Three-way analysis of variance (treatment, time, intensity) was used to determine significant difference. To assess the appropriateness for three-way ANOVA, the normality assumption was assessed

using Normal Quantile Plots and the equality of variance assumption was assessed using Residual Plots. Residuals plots that displayed heterogenous variance were reassessed with a logarithmic transformation. Pooled t-tests were used to identify specific main treatment effect and/or interaction effect. If the variances were still determined to be heterogenous after the logarithmic transformation, analysis proceeded with a Kruskal Wallis Test. Post hoc comparisons were completed with the Mann–Whitney *U* Test. For all analyses, a *p-value* of <0.05 was set as the criteria for significance.

Results

Characterization of generated welding fume

ICP-AES elemental analysis indicated that Cu-Ni fume was primarily Cu and Ni (Figure 1, top left). Cu content by weight percent averaged 76.3% and Ni was 11.6%. Approximately 5% of fume consisted of other metals including Fe, Ti and Mn and the remaining metal content of the fume was trace metals (<1%). Because welding is known to generate a significant number of nanosized particles, both MOUDI and Nano-MOUDI samplers were used to determine particle size distribution. Most of the particles were between 0.1 and 1 μm in diameter, with a mass median aerodynamic diameter of 0.43 μm (Figure 1, top right). SEM-EDS spectral analysis confirmed the ICP-AES results and showed the predominant metal components of the fume were Cu and Ni (Figure 1, bottom left). FESEM image of the generated welding fume that shows primary particles in the nanometer size range linked together in elongated chain-like structures often with several branches (Figure 1, bottom right).

Whole lung metal deposition after Cu-Ni fume inhalation

The lung metal deposition in A/J mice measured at time 0 after 4 hours of inhalation of Cu-Ni fume (average concentration 43 mg/m^3) is shown in Table 1 and was calculated as done previously (Falcone et al. 2017). The most abundant metals measured were Cu (5.11 μg Cu/7.33 μg total metal deposition = 69.7%) and Ni (1.18 μg Ni/7.33 μg total metal deposition = 16.1%), which equates to the elemental analysis of the fume shown in Figure 1.

Human relevance deposition calculation:

The analysis of the metals showed a cumulative increase of 7.33 μg of total Cu-Ni fume deposited in the lung from a single 4 hour exposure (Table 1). The alveolar deposition in the mice was equated to the human by the equations below using the previous threshold limit value-time weighted average (TLV-TWA) of 5 mg/m^3 for total welding fume. Previously, we estimated that 70% of the total deposited dose reached the alveolar space (7.33 μg/d × 0.70 = 5.13 μg/d) (Raabe et al. 1988; Stone et al. 1992; Erdely et al. 2011). Therefore, the Cu-Ni fume was deposited at approximately 1.28 μg/h at 43 mg/m^3. For the pulmonary toxicity studies, mice were exposed for 10 days (2 or 4 hours/day) for an estimated total alveolar deposition of 26 or 51.3 μg, respectively. Because the exposure concentration was on average 23 and 27.3 mg/m^3, for the LD and HD, respectively, over 10 days (versus 4 h at 43 mg/m^3) the total alveolar deposition would be ~13.7 and 32.6 μg per mouse.

Estimated human daily deposition using previous welding fume TLV-TWA of 5 mg/m^3:

Fume concentration × minute volume × exposure duration × deposition efficiency = deposited human dose

$$5\text{mg/m}^3 \times (201/\text{min})\left(10^{-3}\text{m}^3/1\right) \times (8\text{ h/day})(60\text{ min/h}) \times 0.16 = 7.7\text{mg deposited per 8 hour day in humans}$$

Estimated human equivalent deposition of the Cu-Ni LD from quantified deposition in mouse using alveolar surface area (SA) *(Stone et al. 1992)*

$$(\text{SA}_{\text{human}} \times \text{deposition}_{\text{mouse}})/\text{SA}_{\text{mouse}} = \text{deposition}_{\text{human}}$$
$$\left(102\text{ m}^2 \times 0.0137\text{ mg}\right)/0.05\text{ m}^2 = 27.9\text{ mg}$$

27.9 mg/7.7 mg/day = approximately 4 working days for a human working at 5 mg/m^3 for 8 h/day.

Estimated human equivalent deposition of the Cu-Ni HD from quantified deposition in mouse using alveolar SA

$$(\text{SA}_{\text{human}} \times \text{deposition}_{\text{mouse}})/\text{SA}_{\text{mouse}} = \text{deposition}_{\text{human}}$$
$$\left(102\text{ m}^2 \times 0.0326\text{ mg}\right)/0.05\text{ m}^2 = 66.5\text{ mg}$$

66.5 mg/7.7 mg/day = approximately 9 working days for a human working at 5 mg/m^3 for 8 h/day.

Given welding is intermittent work and workplace exposure levels are unlikely to be observed at 5 mg/m^3 for 8 h per day, the estimates of 4 and 9 days would be more representative if referenced as ~32 h and ~72 h for the deposited LD and HD, respectively, for Cu-Ni fume at 5 mg/m^3.

Lung Toxicity parameters

Body weight, cytotoxicity and inflammatory cell influx—At 1 and 7 days post-exposure, Cu-Ni HD fume exposure caused a significant loss of body weight in exposed animals (Figure 2). By 28 days, the Cu-Ni HD group was gaining weight that matched the gain of the air controls by 84 days post-exposure. All Cu-Ni LD post-exposure groups gained weight; however, there was a small, but significant, difference in weight gain compared to air controls at the 1 day timepoint (data not shown).

Lung cytotoxicity, measured as LDH activity in the first fraction acellular BAL fluid, was evident and significant (>12–19 fold change) in both the Cu-Ni fume LD and HD groups at 1 and 7 days post-exposure. The response had decreased, but remained significant, at 28 days (~2 fold change) and returned to control levels by 84 days post-exposure (Figure 3).

Total BAL cells were significantly increased compared to air controls at 1, 7, and 28 days post-exposure to Cu-Ni welding fume LD or HD. By 84 days post-exposure, total cells were slightly, but significantly, increased in the Cu-Ni LD group only. The inflammatory cell increase found at 1 day post-exposure was due to a robust and significant PMN influx (~86% of recovered BAL cells) in both the Cu-Ni fume-exposed LD and HD groups (Figure 4 left and right panel, respectively). By 7 days post-exposure, the inflammatory cell influx had shifted to ~50% macrophages in both exposure groups. The overall lung response by 28 days decreased and the cell profile was >98% macrophages and PMN remained significantly increased (<2%) in both the Cu-Ni LD and HD groups. By 84 days, only the LD group had a small, but significant, increase in PMN (~<1%). Lymphocytes were not a significant component of the lung response to Cu-Ni welding fume exposure. No clear dose-dependency was observed despite half the inhalation exposure duration.

Macrophage phagocytic function—BAL macrophages had a reduced ability to phagocytose *E. coli* 1 and 7 days post-exposure to Cu-Ni LD welding fume (Figure 5). This ability returned to control levels by 28 days. As the cellular influx and cytotoxicity results were similar for both the Cu-Ni LD and HD exposures, only the LD group was analyzed.

Bal fluid cytokine analysis—At 7 days post-exposure several pro-inflammatory proteins were significantly increased in the BAL fluid of Cu-Ni LD and HD welding fume-exposed mice (Figure 6). Many of these cytokines and chemokines are representative of the innate immune response to cytotoxicity as well as cellular signaling eliciting PMN influx and subsequent macrophage accumulation. These included BAL proteins such as G-CSF, IL-6, KC, MCP-1, MIG, MIP-1α, MIP-1β, and TNF-α in the exposed groups. The radar plots shown in Figure 7 illustrate not only a marked response at 7 days post exposure with resolution at 28 days, but also a general overlap in magnitude of response between the LD and HD exposures.

Histopathological analysis—Morphological findings are presented in Table 2 with representative photomicrographs of the findings shown in Figure 8. Alveolar inflammation, chronic-active was found in the right lung of Cu-Ni HD fume-exposed mice terminated on day 1 post-exposure (left panel). This inflammatory lesion was predominantly peribronchiolar to subpleural in distribution, but sometimes involved bronchioles. It ranged from minimal to moderate in severity and consisted of viable and degenerate neutrophils, macrophages, and abundant cellular debris. This lesion was associated with alveolar basophilic globular to granular foreign material (presumptive Cu-Ni particulate matter) in all mice. Minimal hyperplasia of the terminal bronchiolar epithelium, squamous metaplasia or erosion/ulceration in some mice was also noted.

By 7 days post-exposure chronic alveolar inflammation (right panel) was diagnosed in the right lung of all Cu-Ni fume-exposed mice. This lesion was predominantly peribronchiolar to subpleural in distribution, ranged from mild to moderate in severity, and consisted of macrophages with fewer lymphocytes, plasma cells and neutrophils, and abundant cellular debris. It was frequently associated with alveolar basophilic foreign material similar to that observed at 1 day post-exposure. This lesion was variably associated with

minimal hyperplasia of the terminal bronchiolar epithelium or alveolar type II pneumocyte hyperplasia in some mice. Minimal to mild bronchial-associated lymphoid tissue (BALT) hyperplasia was also observed. At 28 and 84 days post-exposure, alveolar macrophage aggregation was seen in the right lung of Cu-Ni fume-exposed mice. This lesion was minimal in severity and consisted of loose aggregates of alveolar macrophages at 28 days then more cohesive aggregates at day 84 post-exposure that sometimes contained rare intracytoplasmic basophilic granular debris (presumptive Cu-Ni particulate matter). Foreign material in the alveolar region was not detected by day 28 suggesting the potential lack of pulmonary persistence of Cu-Ni welding fume. Minimal BALT hyperplasia was also found. There were no visible lesions in the right lung of control mice exposed to air in all study termination groups.

Discussion

The toxicity of MS and SS welding fumes has been extensively characterized and, more recently, the fumes were classified as Group 1 carcinogens by the IARC (IARC Working Group on the Evaluation of Carcinogenic Risk to Humans 2018). This has led to the exploration of newer welding consumables such as the Cu-Ni investigated in the present study. The novel findings were that inhalation of a Cu-Ni welding fume induced marked cytotoxicity, inflammatory cell influx, and an innate immune response in the lung acutely. These lung effects resolved, and no chronic pathology was observed with the exception of minimal macrophage accumulation observed at 84 days post-exposure. Despite half the exposure duration, the pulmonary inflammatory responses were similar between the LD and HD exposures. To our knowledge, this is the first *in vivo* inhalation study investigating a Cu-Ni welding fume where the primary metal component was Cu.

There is no adequate particle comparison to the Cu-Ni fume which has nanosized primary particles of Cu and Ni that condense into chain-like aggregates with an aerodynamic diameter of 0.4 μm. Meaning, the Cu-Ni particulate is similar to other welding fumes in physical dimensions but not similar with respect to specific metals and solubility. Also, there may be some similarity to solubility of Cu nano/micro sized particles, but the physical dimensions will not be the same and the fume is not a single metal. Given the metal composition of the fume was measured to be 76/12/12 for Cu/Ni/other trace metals, respectively, a comparison to Cu nanoparticle was explored in the literature. In the present study weight loss was observed in the Cu-Ni HD group and, consistent with this result, an intranasal delivery of CuO nanoparticles decreased body weight initially even at the lowest deposited dose tested (2.5 mg/kg) (Lai et al. 2018). Regardless of the animal species, CuO nanoparticle exposure resulted in significant acute inflammation including inflammatory cell influx, cellular toxicity, and altered inflammatory signaling with cytokine/chemokine production (Gosens et al. 2016; Costa et al. 2018; Lai et al. 2018; Rossner et al. 2020; Gosens et al. 2021). In particular, CCL2/MCP-1, a monocyte chemoattractant, was a key cytokine involved in the response to the Cu exposure (Costa et al. 2018; Gosens et al. 2021). In line with this finding, CCL2/MCP-1 was also a predominant protein found in the BAL fluid in both Cu-Ni fume exposure groups. Inflammation, the predominant lesion, was observed as an acute response early that progressively resolved by 28 days with only macrophage aggregates remaining late in this study and similarly in others (Gosens et

al. 2016). By day 28, histopathological analysis revealed no particles were present which suggests clearance of the welding fume. Gosens et al. (2021) reported clearance of all CuO nanoparticles within the 21-day recovery period after exposure which was consistent with the histopathological analysis in the present study. No chronic pathology was observed after exposure to Cu-Ni welding fume. However, pathology due to CuO nanoparticle exposure has been reported to result in potential fibrosis in one study whereas others found no long-term effects (Gosens et al. 2016; Lai et al. 2018). The present study design resulted in no structural pathological changes in the lung after Cu-Ni fume exposure. It cannot be excluded that a chronic exposure or a higher level of exposure would not cause pathology. However, this may not be a likely outcome based on the dose extrapolations to the human and somewhat rapid clearance of the particulate.

Ni represents the second largest metal component of the fume tested and is classified as carcinogenic to humans by the IARC, as supported by many worker and animal studies (IARC Working Group on the Evaluation of Carcinogenic Risk to Humans 1990; Costa 1991; Langard 1994; Shen & Zhang 1994; Antonini 2003; Kasprzak et al. 2003). Previous work by our lab has evaluated individual surrogate metal components of SS welding fume which included exposures to nickel oxide (NiO) in mice. NiO, deposited dose of up to 281 ug, caused no lung cytotoxicity, lung inflammation, or tumor promotion (Falcone et al. 2018). This dose of NiO would exceed the amount deposited in the lung in this study by more than an order of magnitude. These results suggest that the acute lung toxicity and inflammation was the result of the Cu component of the welding fume.

The profile of the response to Cu-Ni welding fume differed compared to other fumes examined previously in both rats and mice. For example, inhalation to GMAW-SS fume resulted in significant toxicity and inflammation that began 3 days post-exposure and peaked 10 to14 days post-exposure (Antonini et al. 2007; Zeidler-Erdely et al. 2011). The response to Cu-Ni fume was not delayed, and the animals had significant weight loss and inflammation at 1 day post-exposure through 7 days. Conversely, inhalation of MS welding fumes, despite being a Group 1 carcinogen, does not induce lung toxicity in animal models. Only two published studies have investigated the pneumotoxicity of a fume containing significant amounts of Ni and Cu. Antonini et al. 2014 investigated the pulmonary toxicity of a Ni-Cu fume generated by shielded metal arc welding (SMAW) using both *in vitro* and *in vivo* assays (Antonini et al. 2014; Badding et al. 2014). This complex fume contained twice as much Ni (~13%) than Cu (~6%), a low percentage (<2%) of Cr and Fe, and numerous alkali metals derived from the flux. Intratracheal instillation (2 mg) of this fume in rats caused a greater lung response compared to SS and MS fumes when dosed equally. Interestingly, the Ni-Cu welding fume did not increase reactive oxygen species (ROS), so it was hypothesized by the authors that the toxicity was due to a direct cytotoxic effect. Another study using the same Ni-Cu fume found that it was more cytotoxic than SS or MS fume, causing cell death and mitochondrial dysfunction at lower doses than the other fumes (Badding et al. 2014). Taken together, these studies suggest fumes that contain greater amounts of Cu and Ni may not be ideal for potentially reducing toxic and inflammatory lung effects compared to other, more common, welding consumables.

This study highlights the need for further research on Cu-Ni welding fumes. One aspect that needs addressed is metal solubility, particularly of the Cu component. Welding fume toxicity in the lung appears to be dependent on the interplay of the insoluble and the soluble metal fractions. As shown previously, welding fumes containing soluble metals had increased toxicity compared to other fumes with less solubility (Taylor et al. 2003; Zeidler-Erdely et al. 2008). The results of this study suggest that the Cu-Ni fume likely exhibits a greater acute toxicity that resolves, compared to other welding fumes with metal solubility perhaps being a contributing factor. Additional *in vitro* and *in vivo* and studies are planned to determine effects related to solubility and potential lung carcinogenicity of this fume.

Acknowledgements

The authors thank the NIOSH inhalation and animal quarters staff for their expert assistance with the animal inhalation exposures. We also thank staff toxicologic pathologist Dr. Kristen R. Hobbie, D.V.M., Ph.D., D.A.C.V.P. (Inotiv; West Lafayette, IN) for the interpretation of the histopathology slides.

Funding

This work was supported by the National Institute for Occupational Safety and Health.

Data availability statement

Data will be made available via the NIOSH Gateway.

References

Antonini Mannetje A, Brennan P, Zaridze D, Szeszenia-Dabrowska N, Rudnai P, Lissowska J, Fabianová E, Cassidy A, Mates D, Bencko V, et al. 2012. Welding and lung cancer in Central and Eastern Europe and the United Kingdom. Am J Epidemiol 175(7):706–714. [PubMed: 22343633]

Antonini JM, Afshari AA, Stone S, Chen B, Schwegler-Berry D, Fletcher WG, Goldsmith WT, Vandestouwe KH, McKinney W, Castranova V, et al. 2006. Design, construction, and characterization of a novel robotic welding fume generator and inhalation exposure system for laboratory animals. J Occup Environ Hyg 3(4):194–203. [PubMed: 16531292]

Antonini JM, Badding MA, Meighan TG, Keane M, Leonard SS, Roberts JR. 2014. Evaluation of the pulmonary toxicity of a fume generated from a nickel-, copper-based electrode to be used as a substitute in stainless steel welding. Environ Health Insights 8(Suppl 1):11–20. [PubMed: 25392698]

Antonini JM, Stone S, Roberts JR, Chen B, Schwegler-Berry D, Afshari AA, Frazer DG. 2007. Effect of short-term stainless steel welding fume inhalation exposure on lung inflammation, injury, and defense responses in rats. Toxicol Appl Pharmacol 223(3):234–245. [PubMed: 17706736]

Antonini JM. 2003. Health effects of welding. Crit Rev Toxicol. 33(1): 61–103. [PubMed: 12585507]

Badding MA, Fix NR, Antonini JM, Leonard SS. 2014. A comparison of cytotoxicity and oxidative stress from welding fumes generated with a new nickel-, copper-based consumable versus mild and stainless steel-based welding in RAW 264.7 mouse macrophages. PLoS One 9(6):e101310. [PubMed: 24977413]

Coggon D, Inskip H, Winter P, Pannett B. 1994. Lobar pneumonia: an occupational disease in welders. Lancet 344(8914):41–43. [PubMed: 7912307]

Costa M. 1991. Molecular mechanisms of nickel carcinogenesis. Annu Rev Pharmacol Toxicol 31:321–337. [PubMed: 2064378]

Costa PM, Gosens I, Williams A, Farcal L, Pantano D, Brown DM, Stone V, Cassee FR, Halappanavar S, Fadeel B. 2018. Transcriptional profiling reveals gene expression changes associated with inflammation and cell proliferation following short-term inhalation exposure to copper oxide nanoparticles . J Appl Toxicol 38(3):385–397. [PubMed: 29094763]

Driscoll KE, Lindenschmidt RC, Maurer JK, Higgins JM, Ridder G. 1990. Pulmonary response to silica or titanium dioxide: inflammatory cells, alveolar macrophage-derived cytokines, and histopathology. Am J Respir Cell Mol Biol 2(4):381–390. [PubMed: 2157474]

Erdely A, Hulderman T, Salmen-Muniz R, Liston A, Zeidler-Erdely PC, Chen BT, Stone S, Frazer DG, Antonini JM, Simeonova PP. 2011. Inhalation exposure of gas-metal arc stainless steel welding fume increased atherosclerotic lesions in apolipoprotein E knockout mice. Toxicol Lett 204(1):12–16. [PubMed: 21513782]

Falcone LM, Erdely A, Meighan TG, Battelli LA, Salmen R, McKinney W, Stone S, Cumpston A, Cumpston J, Andrews RN, et al. 2017. Inhalation of gas metal arc-stainless steel welding fume promotes lung tumorigenesis in A/J mice. Arch Toxicol. 91(8):2953–2962. [PubMed: 28054104]

Falcone LM, Erdely A, Salmen R, Keane M, Battelli L, Kodali V, Bowers L, Stefaniak AB, Kashon ML, Antonini JM, et al. 2018. Pulmonary toxicity and lung tumorigenic potential of surrogate metal oxides in gas metal arc welding-stainless steel fume: iron as a primary mediator versus chromium and nickel. PLoS One 13(12): e0209413. [PubMed: 30586399]

Gosens I, Cassee FR, Zanella M, Manodori L, Brunelli A, Costa AL, Bokkers BGH, de Jong WH, Brown D, Hristozov D, et al. 2016. Organ burden and pulmonary toxicity of nano-sized copper (II) oxide particles after short-term inhalation exposure. Nanotoxicology 10(8):1084–1095. [PubMed: 27132941]

Gosens I, Pedro M, Costa PM, Olsson M, Stone V, Costa AL, Brunelli A, Badetti E, Bonetto A, Bokkers BGH, et al. 2021. Pulmonary toxicity and gene expression changes after short-term inhalation exposure to surface-modified copper oxide nanoparticles. Nanoimpact 22:100313. [PubMed: 35559970]

Holm M, Kim J-L, Lillienberg L, Storaas T, Jogi R, Svanes C, Schlunssen V, Forsberg B, Gislason T, Janson C, et al. 2012. Incidence and prevalence of chronic bronchitis: impact of smoking and welding. The RHINE study. Int J Tuberc Lung Dis 16(4): 553–557. [PubMed: 22325166]

IARC Working Group on the Evaluation of Carcinogenic Risk to Humans, 2012. Arsenic, metals, fibres, and dusts. IARC Monogr Eval Carcinog Risks Hum 100(Pt C):11–465. [PubMed: 23189751]

IARC Working Group on the Evaluation of Carcinogenic Risk to Humans, 1990. Chromium, nickel and welding. IARC Monogr. Eval Carcinog Risks Hum 49:1–648. [PubMed: 2232124]

IARC Working Group on the Evaluation of Carcinogenic Risk to Humans, 2018. Welding, molybdenum trioxide, and indium tin oxide. IARC Monogr Eval Carcinog 118:37–263.

Kasprzak KS, Sunderman FW Jr, Salnikow K. 2003. Nickel carcinogenesis. Mutat Res 533(1–2):67–97. [PubMed: 14643413]

Kodali VK, Roberts JR, Shoeb M, Wolfarth MG, Bishop L, Eye T, Barger M, Roach KA, Friend S, Schwegler-Berry D, et al. 2017. Acute in vitro and in vivo toxicity of a commercial grade boron nitride nanotube mixture. Nanotoxicology 11(8):1040–1058. [PubMed: 29094619]

Lai X, Zhao H, Zhang Y, Guo K, Xu Y, Chen S, Zhang J. 2018. Intranasal delivery of cooper oxide nanoparticles induces pulmonary toxicity and fibrosis in C57BL/6 mice. Sci. Rep 8:4499. [PubMed: 29540716]

Langard S. 1994. Nickel-related cancer in welders. Science Total Environ 148(2–3):303–309.

Ma JY, Zhao H, Mercer RR, Barger M, Rao M, Meighan T, Schwegler-Berry D, Castranova V, Ma JK. 2011. Cerium oxide nanoparticle-induced pulmonary inflammation and alveolar macrophage functional change in rats. Nanotoxicology 5(3):312–325. [PubMed: 20925443]

Mann PC, Vahle J, Keenan CM, Baker JF, Bradley AE, Goodman DG, Harada T, Herbert R, Kaufmann W, Kellner R, et al. 2012. International harmonization of toxicologic pathology nomenclature: an overview and review of basic principles. Toxicol Pathol 40(4 Suppl):7S–13S.

Marongiu A, Hasan O, Ali A, Bakhsh S, George B, Irfan N, Minelli C, Canova C, Schofield S, De Matteis S, et al. 2016. Are welders more at risk of respiratory infections? Findings from a cross-sectional survey and analysis of medical records in shipyard workers: the WELSHIP project. Thorax 71(7):601–606. [PubMed: 27030577]

Matrat M, Guida F, Mattei F, Cénée S, Cyr D, Févotte J, Sanchez M, Menvielle G, Radoï L, Schmaus A, ICARE Study Group, et al. 2016. Welding, a risk factor of lung cancer: the ICARE study. Occup Environ Med 73(4):254–261. [PubMed: 26865654]

NIOSH 1994. Method 7303, Elements by ICP (Hot Block/HCl/HNO3 digestion). In: NIOSH manual of analytical methods, 4th ed., Issue 2. Washington, DC: U.S. Department of Health and Human Services, Publication No. 98–119. https://www.cdc.gov/niosh/nmam/.

NIOSH 2018. Method 8200, Elements in Tissues. In: Andrews RN, O'Connor PF, eds. NIOSH manual of analytical methods 5th ed. Cincinnati, OH: U.S. Department of Health and Human Services, Centers for Disease Control and Prevention, National Institute for Occupational Safety and Health, DHHS (NIOSH) Publication No. 2014–151. https://www.cdc.gov/niosh/nmam/.

Raabe OG, Al-Bayati MA, Teague SV, Rasolt A. 1988. Regional deposition of inhaled monodisperse coarse and fine aerosol particles in small laboratory animals. Ann Occup Hyg 32:53–63.

Renne R, Brix A, Harkema J, Herbert R, Kittel B, Lewis D, March T, Nagano K, Pino M, Rittinghausen S, et al. 2009. Proliferative and nonproliferative lesions of the rat and mouse respiratory tract. Toxicol Pathol 37(7 Suppl):5S–73S. [PubMed: 20032296]

Rossner P Jr, Vrbova, Rossnerova A, Zavodna T, Milcova A, Klema J, Vecera Z, Mikuska P, Coufalik P, Capka L, et al. 2020. Gene expression and epigenetic changes in mice following inhalation of copper(II) oxide nanoparticles. Nanomaterials 10(3):550. [PubMed: 32197515]

Shen HM, Zhang QF. 1994. Risk assessment of nickel carcinogenicity and occupational lung cancer. Environ Health Perspect 102 Suppl 1(Suppl 1):275–282.

Siew SS, Kauppinen T, Kyyronen P, Heikkila P, Pukkala E. 2008. Exposure to iron and welding fumes and the risk of lung cancer. Scand J Work Environ Health 34(6):444–450. [PubMed: 19137206]

Sorensen AR, Thulstrup AM, Hansen J, Ramlau-Hansen CH, Meersohn A, Skytthe A, Bonde JP. 2007. Risk of lung cancer according to mild steel and stainless steel welding. Scand J Work Environ Health 33(5):379–386. [PubMed: 17973064]

Stone KC, Mercer RR, Gehr P, Stockstill B, Crapo JD. 1992. Allometric relationships of cell numbers and size in the mammalian lung. Am J Respir Cell Mol Biol 6(2):235–243. [PubMed: 1540387]

Suri R, Periselneris J, Lanone S, Zeidler-Erdely PC, Melton G, Palmer KT, Andujar P, Antonini JM, Cohignac V, Erdely A, et al. 2016. Exposure to welding fumes and lower airway infection with Streptococcus pneumoniae. J Allergy Clin Immunol 137(2): 527–534. [PubMed: 26277596]

Taylor MD, Roberts JR, Leonard SS, Shi X, Antonini JM. 2003. Effects of welding fumes of differing composition and solubility on free radical production and acute lung injury and inflammation in rats. Toxicol Sci 75(1):181–191. [PubMed: 12832661]

Yang H-M, Barger MW, Castranova V, Ma JKH, Yang J-J, Ma JYC. 1999. Effects of diesel exhaust particles (DEP), carbon black, and silica on macrophage responses to lipopolysaccharide: evidence of DEP suppression of macrophage activity. J. Toxicol. Environ. Health Part A 58(5):261–278.

Zeidler-Erdely PC, Battelli LA, Stone S, Chen BT, Frazer DG, Young S-H, Erdely A, Kashon ML, Andrews R, Antonini JM. 2011. Short-term inhalation of stainless steel welding fume causes sustained lung toxicity but no tumorigenesis in lung tumor susceptible A/J mice. Inhal Toxicol 23(2):112–120. [PubMed: 21309664]

Zeidler-Erdely PC, Kashon ML, Battelli LA, Young S-H, Erdely A, Roberts JR, Reynolds SH, Antonini JM. 2008. Pulmonary inflammation and tumor induction in lung tumor susceptible A/J and resistant C57BL/6J mice exposed to welding fume. Part Fibre Toxicol 5:12. [PubMed: 18778475]

Zeidler-Erdely PC, Meighan TG, Erdely A, Battelli LA, Kashon ML, Keane M, Antonini JM. 2013. Lung tumor promotion by chromium-containing welding particulate matter in a mouse model. Part Fibre Toxicol 10(1):45. [PubMed: 24107379]

Metals	Weight % of Metals
Cu	76.3
Ni	11.6
Fe	5.10
Ti	2.90
Mn	2.30

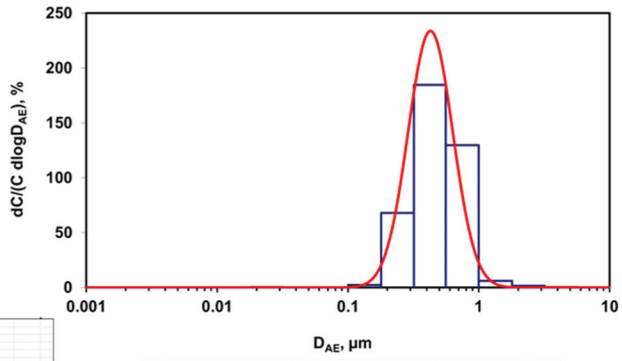

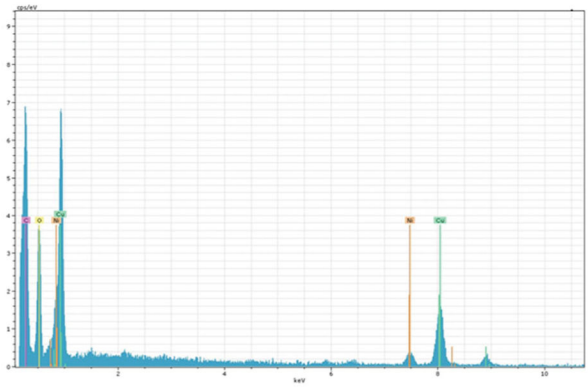

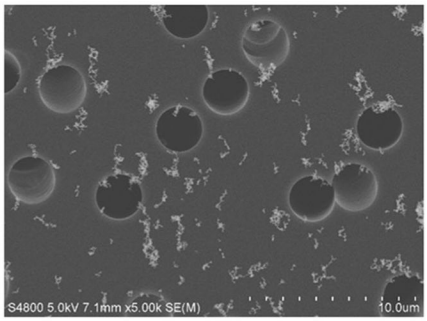

Figure 1.

Top left panel - The generated welding fume was analyzed by ICP-AES. Weight % is relative to all metals analyzed. Values are mean ± standard error of the mean ($n = 3$ welding fume collection periods of 30 min). Top right panel - Particle size distribution of the generated welding fume measured using the MOUDI and Nano-MOUDI impactor systems (C = mass concentration and D_{AE} = aerodynamic diameter). Bottom left panel – SEM-EDS analysis of the generated fume. The labeled thin vertical lines are guidelines to the positions of the spectral peaks for the elements. Bottom right panel – FESEM image of the generated welding fume.

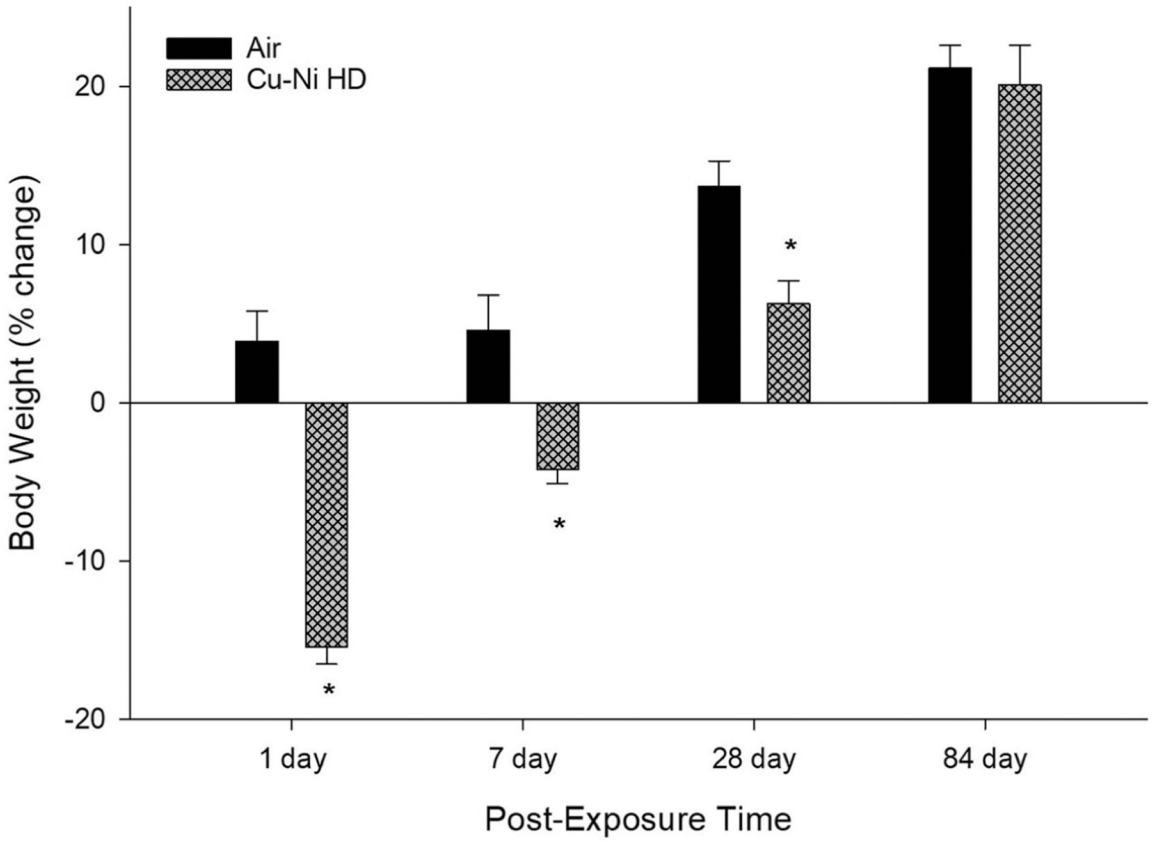

Figure 2.

Body weight changes at 1,7,28, and 84 days post-exposure to Cu-Ni welding fume HD ($n = 15–16$) or filtered air (control; $n = 15–16$). Data presented as percent change from pre-exposure body weight. *$p < 0.05$ compared to air control.

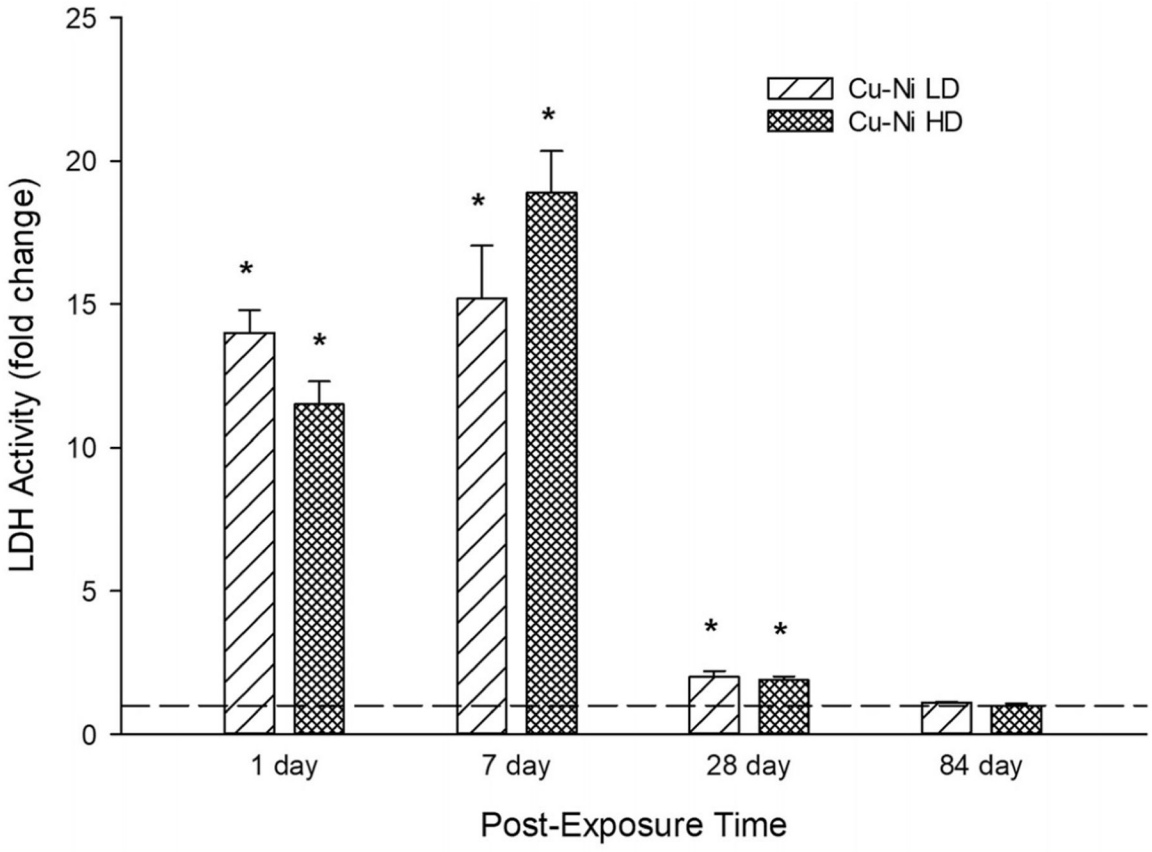

Figure 3.

LDH activity, measured in the BAL fluid and indicative of lung cytotoxicity, at 1,7,28, and 84 days post-exposure to Cu-Ni LD ($n = 7–8$) or HD ($n = 9–11$) welding fume or filtered air (control; $n = 7–8$ for LD and $n = 10–11$ for HD). Data presented as fold change from control (dashed line – 1). *$p < 0.05$ compared to air control.

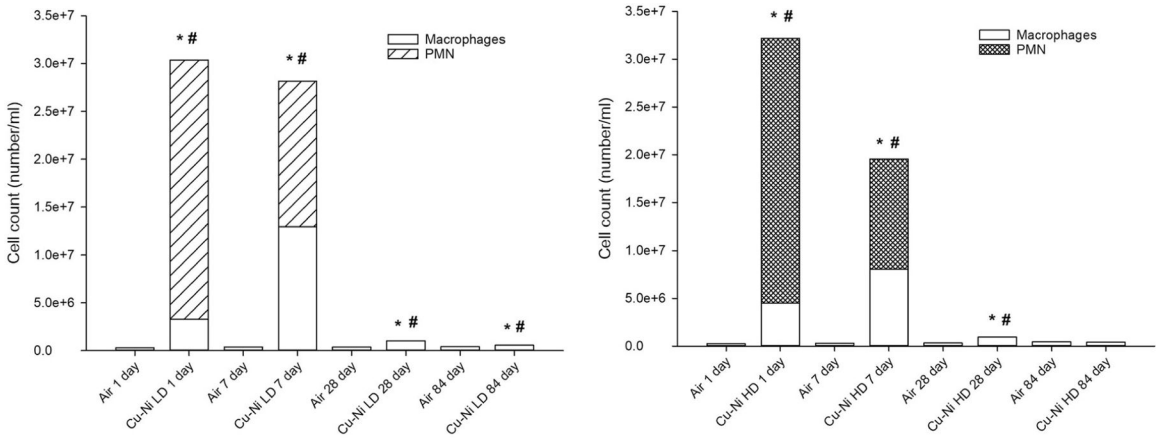

Figure 4.

BAL cellular influx, consisting of macrophages and PMN, at 1,7,28, and 84 days post-exposure to Cu-Ni LD (left panel) or HD (right panel) welding fume exposure. Air exposed control groups [$n = 7–8$ (LD) and $n = 10–11$(HD)] were ~100% macrophages at all timepoints. *$p < 0.05$ compared to control for macrophages; #$p < 0.05$ compared to control for PMN.

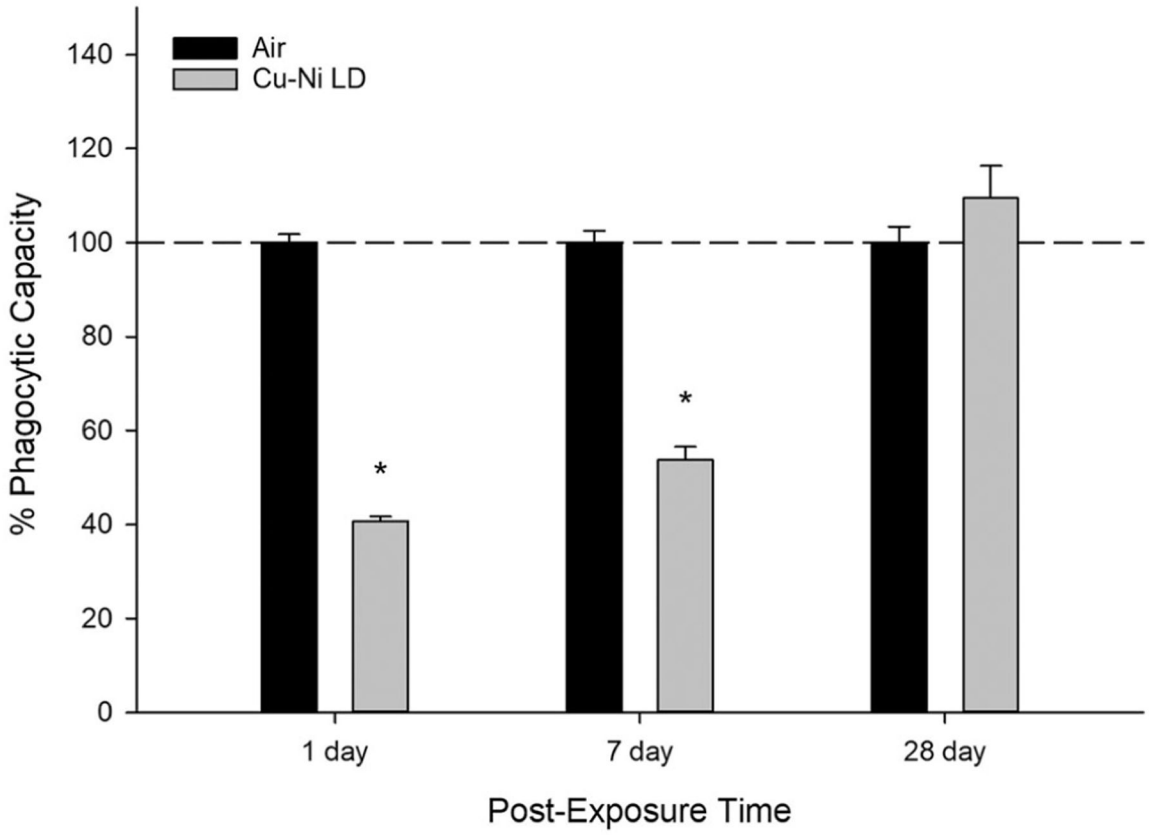

Figure 5.

Ability of alveolar macrophages to phagocytose *E. coli* GFP at 1,7, and 28 days post-exposure to Cu-Ni welding fume for 2 h/day for 10 days at 23 mg/m^3 (LD) or air. *E. coli* uptake by macrophages was quantified by flow cytometry. Data presented as percent change from air control (dashed line – 100%). *$p < 0.05$ compared to air control.

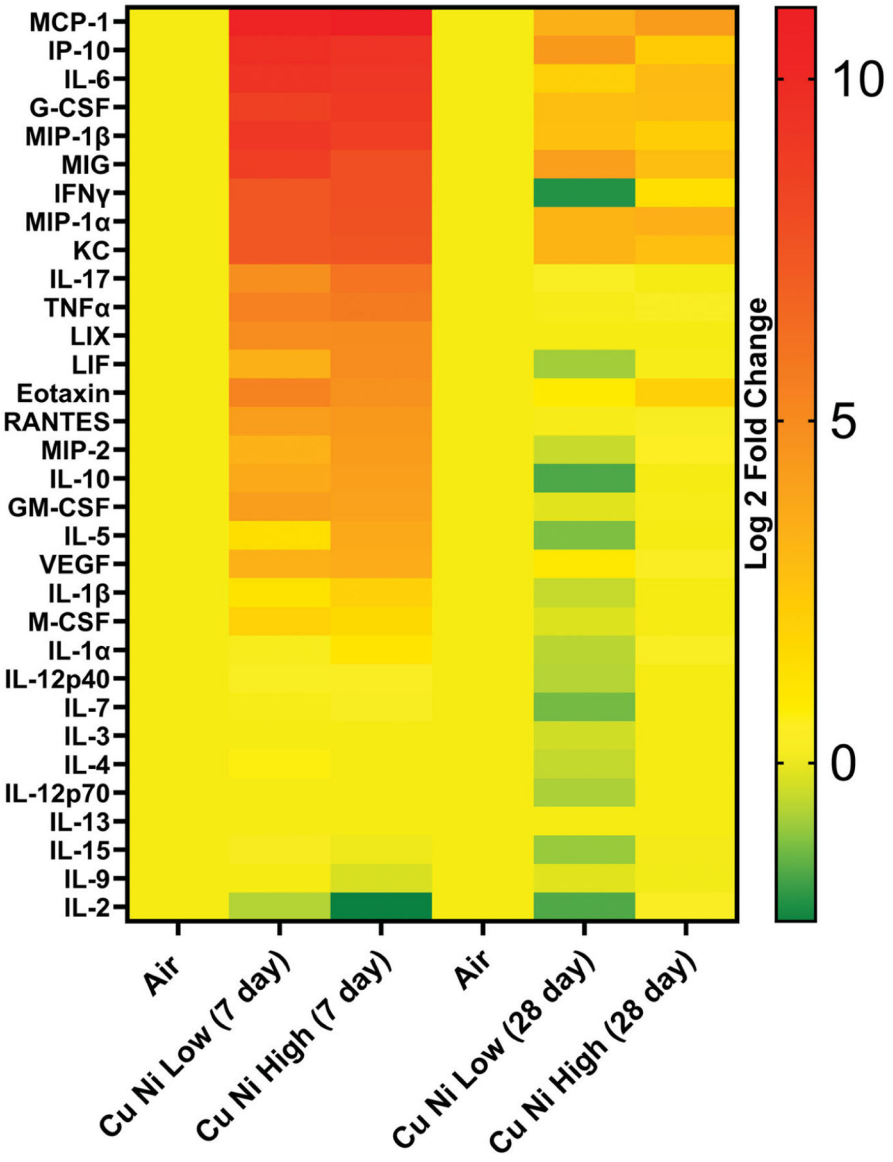

Figure 6.

Heat Map showing BAL fluid protein expression at 7 and 28 days after inhalation exposure to Cu-Ni LD or HD welding fume or filtered air for 10 days. The data is plotted as log2 fold change from protein levels in control animals exposed to filtered air.

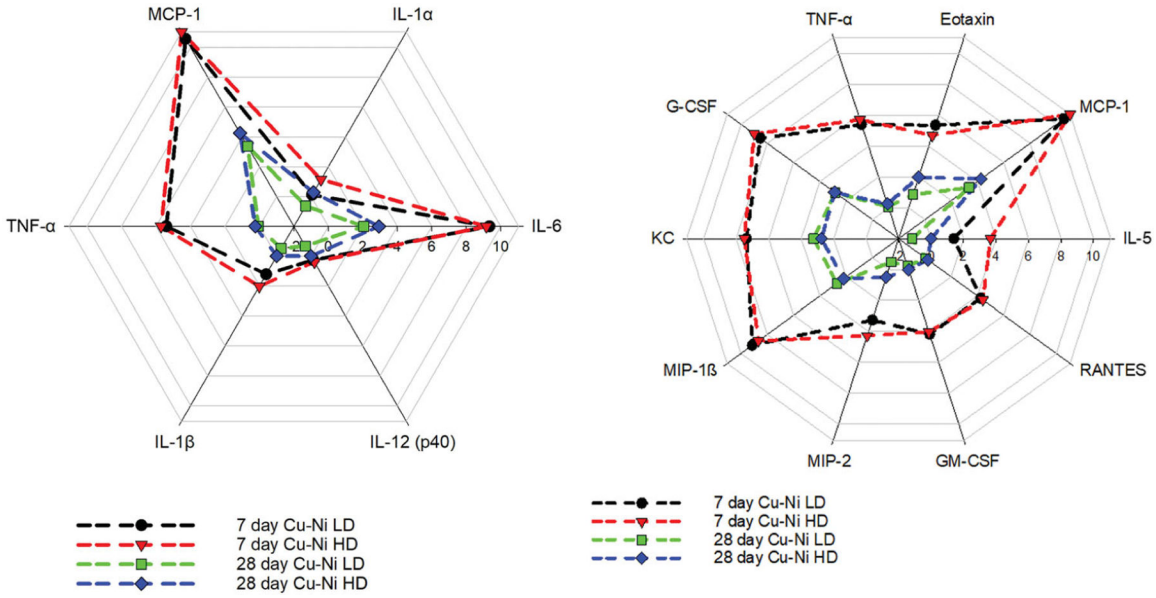

Figure 7.

Multivariant radar charts comparing protein expression patterns in BAL fluid responsible for PMN Influx (left panel) and pro-inflammation (right panel). Both Cu-Ni welding fume LD ($n = 7$–8) and HD ($n = 10$) exposure caused similar patterns of protein expression for PMN influx and pro-inflammation. The level of protein expression decreased over time from day 7 to day 28.

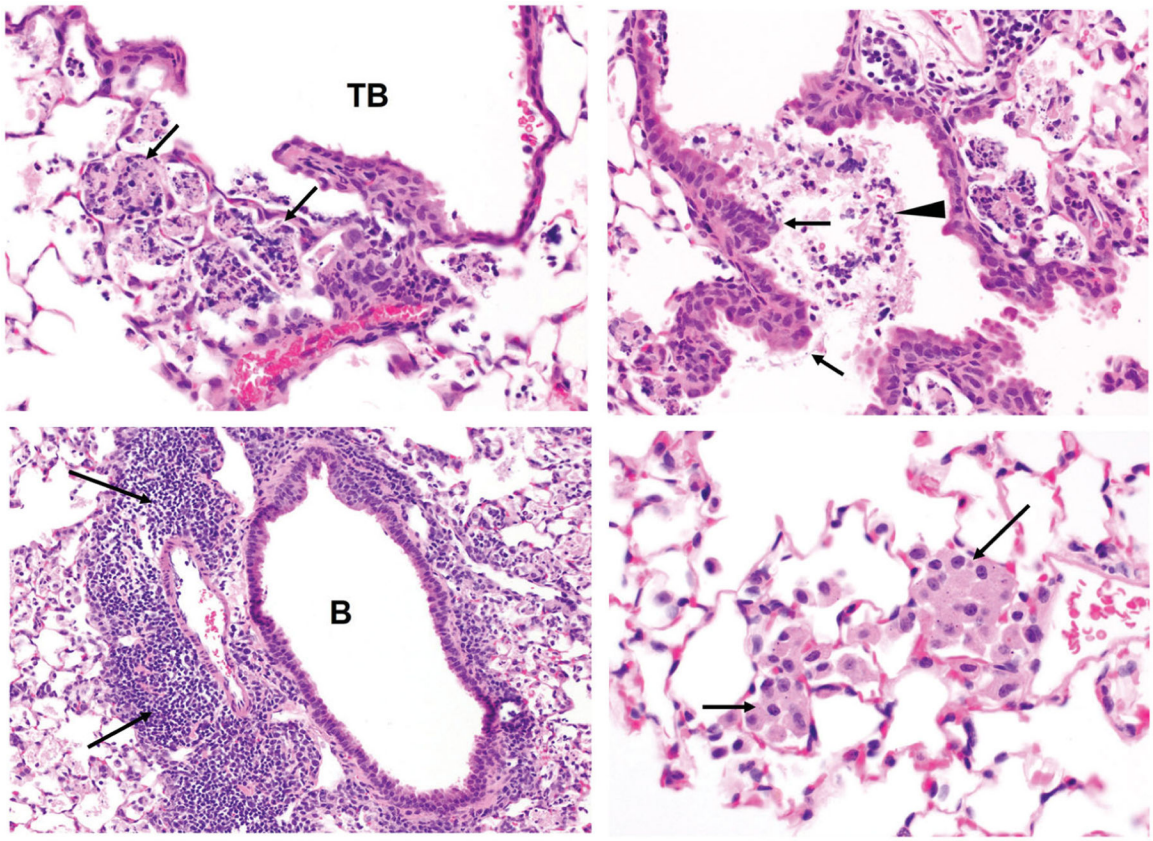

Figure 8.

Upper left - Representative photomicrograph of chronic-active inflammation (black arrows) in alveoli adjacent to a terminal bronchiole (TB) in a Cu-Ni welding fume-exposed mouse lung at 1 day post-exposure (40×). Upper right - Hyperplasia of bronchiolar epithelium (black arrows) associated with inflammation (arrowhead) at 1 day post-exposure (40×). Lower left - Alveolar inflammation, chronic and hyperplasia of bronchiole-associated lymphoid tissue (black arrows) next to a bronchiole (B) at 7 days post-exposure to Cu-Ni welding fume (20×). Lower right - Alveolar macrophage aggregate (black arrows) with rare intracytoplasmic granular material at 84 days post-exposure (60×).

Table 1.

Lung metal deposition in A/J mice after air or Cu-Ni welding aerosol inhalation for 4 h at a concentration of 43.2 mg/m^3.

Exposure	Cu (μg/lung)	Ni (μg/lung)	Fe (μg/lung)	Ti (μg/lung)	Mn (μg/lung)
Air	0.30 ± 0.01	0.05 ± 0.02	9.95 ± 0.35	0.04 ± 0.02	0.03 ± 0.00
Cu-Ni	5.40 ± 0.17	1.23 ± 0.07	10.74 ± 0.27	0.16 ± 0.03	0.16 ± 0.00

Freeze-dried whole lung tissue was analyzed for aluminum (Al), barium (Ba), calcium (Ca), chromium (Cr), cobalt (Co), copper (Cu), iron (Fe), potassium (K), lithium (Li), manganese (Mn), magnesium (Mg), nickel (Ni), phosphorus (P), lead (Pb), strontium (Sr), titanium (Ti), vanadium (V), zinc (Zn), and zirconium (Zr) by Inductively Coupled Plasma-Atomic Emission Spectroscopy. Levels of Al, Ba, Ca, Co, Cr, Li, Mg, P, Pb, Sr, V, Zn and Zr were not included because they were not detectable, <0.1% in the fume analysis, or not significantly higher in exposed animals. *Note*: Values are mean ± standard error of the mean (n = 6 air; n = 10 Cu-Ni).

Table 2.

Severity scores for abnormal morphological findings in right lung of A/J mice exposed to high deposition Cu-Ni welding aerosols.

Day	Exposure	Alveolus; inflammation; chronic	Alveolus; inflammation; chronic-active	BALT; hyperplasia	Bronchiole; epithelium; hyperplasia	Alveolus; foreign material	Alveolus; macrophage aggregation
1	Air	–	0± 0	0 ±0	0±0	0/4	–
	Cu-Ni	–	2.0 ± 0.32 *	0.40 ± 0.24	0.8 ± 0.20 *	5/5	–
7	Air	0 ± 0	–	0 ± 0	0 ± 0	0/6	–
	Cu-Ni	1.8 ± 0.31 *	–	1.2 ± 0.31 *	0.17 ± 0.17	4/6	–
28	Air	0 ± 0	–	0± 0	–	0/6	0 ± 0
	Cu-Ni	0.33 ± 0.21	–	1.0 ± 0.26 *	–	0/6	0.67 ± 0.21 *
84	Air	–	–	–	–	0/6	0 ± 0
	Cu-Ni	–	–	–	–	0/6	1.2 ± 0.17 *

Severity scores for the right lung lobes are presented as mean ± standard error. Severity was scored as: 1: minimal; 2: mild; 3: moderate; 4: marked. – indicates no visible lesion

* $p < 0.03$ – compared to air controls. Day 1 post-exposure (air $n = 4$; Cu-Ni $n = 5$); Days 7,28,84 post-exposure (air $n = 6$; Cu-Ni $n = 6$). Cu-Ni: Copper-Nickel; BALT: bronchial-associated lymphoid tissue.